HEP'99 # 6_430
Submitted to Pa 6
Pl 6

DELPHI 99-69 CONF 256
15 June 1999

OPEN-99-421
15/06/1999

CERN

Measurement of the $Z^0 Z^0$ cross-section in $e^+ e^-$ interactions at 189 GeV

Preliminary

DELPHI Collaboration

Measurement of the Z^0Z^0 cross-section in e^+e^- interactions at 189 GeV

DELPHI PRELIMINARY

R. Jacobsson, C. Parkes
CERN
R. Contri
INFN Genova
R. Keränen
Inst. für Exper. Kernphysik, Karlsruhe
K. Cieslik, H. Palka, M. Witek
Institute of Nuclear Physics, Krakow (supported in part by KBN Grant 2 P03B 111 16)
I. van Vulpen
NIKHEF, Amsterdam
P. Bambade, G. Borisov, E. Ferrer Ribas, S. Gamblin, A. Stocchi
LAL, Orsay
J. Palacios
Nuclear Physics Laboratory, Oxford
H. Carvalho, M. E. Pol
CBPF, Rio De Janeiro
M. Barbi, M. Begalli, J.R.P. Mahon, L.M. Mundim
UERJ, Rio De Janeiro
H.T. Phillips
Rutherford Appleton Laboratory, Didcot
J. Cuevas
Universidad de Oviedo, Oviedo
J. Marco
Instituto de Fisica de Cantabria, CSIC, Spain
A. Ballestrero
INFN Torino

Abstract

In this paper we present measurements of the selected numbers of events found in DELPHI data taken at a centre-of-mass energy of 188.6 GeV in 1998 in the four-fermion final states $l^+l^-l^+l^-$ (excluding $\tau^+\tau^-\tau^+\tau^-$), $e^+e^-q\bar{q}$, $\mu^+\mu^-q\bar{q}$, $\nu\bar{\nu}q\bar{q}$ and $b\bar{b}q\bar{q}$. We interpret these measurements in terms of the cross-section for on-shell Z^0Z^0 production via the tree-level doubly-resonant production graphs (the NC02 graphs) and find $\sigma_{NC02} = 0.58 \pm 0.17$ pb, where the quoted error is statistical only.

1   Introduction

The Z^0 boson has been extensively studied running at the Z pole by LEP1 and SLC and its properties and branching ratios are well known. At higher centre-of-mass energies, it becomes possible to produce pairs of Z^0 bosons, which then decay into fermion-antifermion pairs, giving a four-fermion final state. As the Z^0 has been so well measured, the rate of Z^0Z^0 production and decay into different channels should be well predicted by the Standard Model. It is therefore interesting to check these predictions, particularly as Z^0Z^0 production forms an irreducible background to HZ^0 production if the Higgs has approximately the same mass as the Z^0.

In this paper we present measurements of the selected numbers of events in four-fermion final states $l^+l^-l^+l^-$, $l^+l^-q\bar{q}$, $\nu\bar{\nu}q\bar{q}$ and $b\bar{b}q\bar{q}$ in a mass window of $M_Z \pm 10$ GeV/c^2. We interpret these measurements in terms of the cross-section for on-shell Z^0Z^0 production via the tree level doubly-resonant production graphs (the NC02 graphs).

2   The DELPHI Detector

A summary of the properties of the DELPHI detector relevant to this analysis is presented below. A more detailed description can be found in [1].

Charged particle tracks were measured in a system of cylindrical tracking chambers immersed in a 1.2 T magnetic field. These were the Microvertex Detector, the Inner Detector, the Time Projection Chamber, and the Outer Detector. In addition, two planes of drift chambers aligned perpendicular to the beam axis (Forward Chambers A and B) tracked particles in the forward and backward directions, covering polar angles $11° < \theta < 33°$ and $147° < \theta < 169°$.

The electromagnetic calorimetry consisted of the High density Projection Chamber covering the barrel region of $40° < \theta < 140°$, the Forward Electromagnetic Calorimeter covering $11° < \theta < 36°$ and $144° < \theta < 169°$ and the STIC, a scintillator tile calorimeter which extends the coverage down to $1.66°$ in the forward and backward regions. The $40°$ taggers were a series of single-layer lead-scintillator counters used to veto electromagnetic particles otherwise missed in a region between the barrel and forward calorimeters. The hadron calorimeter covered 98% of the solid angle. Muons with momenta above 2 GeV can pass through the hadron calorimeter; these were recorded in a set of Muon Drift Chambers.

3   Data Sample

DELPHI took data corresponding to an integrated luminosity of 158 pb^{-1} at a centre-of-mass energy of 188.6 GeV in 1998.

Simulated events were produced with the DELPHI simulation program `DELSIM`[2] and then passed through the same reconstruction chain as the data. Processes leading to four-fermion final states were generated with `EXCALIBUR`[3], relying on `JETSET` 7.4 [4] for quark fragmentation. `EXCALIBUR` includes all tree-level diagrams in a consistent fashion. Initial state radiation was treated using the QEDPS program[5] for those final states which did not include e^+e^- pairs; for final states including e^+e^- the default `EXCALIBUR` collinear treatment was used. The `WPHACT` generator[6] was used as a cross-check.

The background processes $e^+e^- \rightarrow f\bar{f}(+n\gamma)$ were generated using PYTHIA[4]. PYTHIA was also used to generate four-fermion final states via the processes $(Z^0/\gamma)^*(Z^0/\gamma)^*$, W^+W^-, $We\nu_e$ and $Z^0e^+e^-$ which were used to cross-check EXCALIBUR. The part of the $e\nu q\bar{q}$ phase space in which the finite electron mass is relevant was simulated with the GRC4F generator[7] in which fermion mass effects are included. PYTHIA does not include all tree-level diagrams so the above processes must be added incoherently. However, it does have an approximate treatment of the transverse momentum of initial state radiation photons for all final states. Two-photon interactions were generated using TWOGAM [8] and BDK [9].

3.1   Signal definition

In the simulation, an event was defined as being a signal event if two pairings of final-state fermions had a generated mass within ± 10 GeV/c^2 of the nominal Z mass, taken to be 91.187 GeV/c^2 [10]. Events with the correct flavour composition but which fell outside this generator-level mass window were considered as background for the purposes of this analysis, which considers on-shell ZZ production. As there are other four-fermion production diagrams which can contribute even in this mass window, a scale factor R,

$$R = \sigma_{NC02}(total)/\sigma_{4f}(window),\qquad(1)$$

was calculated using EXCALIBUR and checked with WPHACT. The selected number of events was used, together with the selection efficiency and background rate which were estimated using the simulation, to calculate the total four-fermion cross-section within the mass window, $\sigma_{4f}(window)$. The scale factor R was then used to convert this to the total NC02 cross-section, $\sigma_{NC02}(total)$.

This procedure defines the on-shell signal by a generator-level cut. In order to select such events in the data, similar cuts must be applied to the measured masses. However, as the mass resolution is different in the different channels, different reconstructed mass windows were used for each channel.

A different method was used to obtain the NC02 cross-section for the $l^+l^-l^+l^-$ channel. Two $l^+l^-l^+l^-$ samples were generated, the first using NC02 graphs only and the second using all other tree-level graphs, with NC02 excluded. The first sample was used to define the signal and the second was used to estimate the background from other four-fermion processes. This procedure neglects interference terms between the NC02 diagrams and the other four-fermion diagrams but as the predicted signal is of order one event this does not have a significant effect. The NC02 cross-section for $l^+l^-l^+l^-$ was then estimated according to the formula:

$$\sigma_{NC02} = \frac{N^{data} - N^{bkg}}{eff \times Lum \times BF(Z^0Z^0 \rightarrow l^+l^-l^+l^-)},\qquad(2)$$

where N^{data} is the number of events selected in the data, N^{bkg} is the number of background events predicted by the simulation, eff is the selection efficiency for the pure NC02 sample, Lum is the integrated luminosity and $BF(Z^0Z^0 \rightarrow l^+l^-l^+l^-) = 0.00939$ is the EXCALIBUR prediction for the branching ratio of ZZ to four charged leptons (excluding four taus).

4 Four charged leptons: $l^+l^-l^+l^-$ Channel

Due to the relatively low branching fraction $BF(Z^0 \to l^+l^-) \simeq 0.1$, only about 1 % of all Z^0Z^0 events lead to the $l^+l^-l^+l^-$ final state. Hence only about one $l^+l^-l^+l^-$ event is predicted in the 1998 data. These events have a clean topology and the only significant background comes from non-resonant $e^+e^-l^+l^-$ production. Since our selection is not sensitive to the $\tau^+\tau^-\tau^+\tau^-$ final state, in the following we use $l^+l^-l^+l^-$ to represent the five other four-lepton final states: $e^+e^-e^+e^-$, $e^+e^-\mu^+\mu^-$, $e^+e^-\tau^+\tau^-$, $\mu^+\mu^-\mu^+\mu^-$ and $\mu^+\mu^-\tau^+\tau^-$.

4.1 Event Selection

The event selection proceeded as follows. The invariant mass of the charged particles was required to be greater than 50 GeV/c^2 and the minimum invariant mass after discarding any one of the charged particles was required to exceed 20 GeV/c^2. The event was required to contain between 4 and 10 charged particles. The number of charged particles with momentum greater than 5 GeV/c should be 3,4,5 or 6. Then all combinations of 4 charged particles with total charge zero were examined:

- at least 3 of the four charged particles must have momenta greater than 5 GeV/c (the fourth track was allowed to have momentum as low as 2 GeV);

- two oppositely-charged particles were required to have both invariant mass and recoil mass within 10 GeV/c^2 of the Z boson mass and the angle of those particles with respect to the beam direction was required to be bigger than 25° in order to ensure that their momentum was well-measured;

- the two additional particles which were supposed to come from the second Z decay were required to be separated by at least 90° from each other;

- the invariant mass of any pair of charged particles was required to exceed 2 GeV/c^2.

No particle identification was demanded in the initial selection but if two identified particles were found with invariant mass close to Z^0 mass, they were required to have the same flavour i.e. e^+e^- or $\mu^+\mu^-$.

4.2 Results

A single event was observed, with a predicted signal of 0.6 events and a predicted background of 0.3 events.

5 $l^+l^-q\bar{q}$ Channel $(l = \mu, e)$

5.1 Event Selection

The selection procedure for the $\mu^+\mu^-q\bar{q}$ and $e^+e^-q\bar{q}$ channels is almost the same and differs mainly in the numerical values of applied cuts.

Events were required to have at least 6 charged particles and a charged energy above $0.30\ \sqrt{s}$. Any charged particle with a momentum exceeding 5 GeV/c was considered as

a possible lepton candidate. Any neutral particle identified as a photon by the DELPHI reconstruction program with an energy of more than 2 GeV was combined with a lepton candidate if the mass of the obtained cluster did not exceed 0.4 GeV/c^2. At most 2 photons were included in such a cluster; the photon giving the smallest mass increase was added first. This procedure allowed association of the lepton candidate with photons from the final state radiation and, in the case of electrons, with photons coming from from interactions with the material in the detector.

The direction of the lepton candidate was determined from the sum of momenta of the particles included in the cluster and the energy was taken to be the sum of their energies. For electron candidates the value used for the energy of the charged particle was the greater of the energy deposited in the electromagnetic calorimeter and the momentum measured by the tracking system.

Events with at least two lepton candidates of the same flavour, opposite charge and invariant mass exceeding 2 GeV/c^2 were selected. All particles except the lepton candidates were clustered into jets using the JADE algorithm [11] with $y_{min} = 0.01$. A kinematic fit [12] including four-momentum conservation was applied to the event. Two discriminating variables for the selection of $l^+l^-q\bar{q}$ final state were defined, namely the transverse momentum, P_t, of a lepton candidate with respect to the nearest jet and the χ^2 per degree of freedom of the kinematic fit.

Among two lepton candidates at least one of them was required to satisfy strong identification criteria and the other was required to satisfy softer identification criteria.

The strong identification criteria for muons were:

- momentum of the charged particle in the cluster exceeds 5 GeV/c;

- particle is identified as a muon by the standard DELPHI identification package [1].

The soft identification criteria for muons were:

- momentum of the charged particle in the cluster exceeds 15 GeV/c;

- energy deposited in the electromagnetic calorimeter does not exceed 30% of the charged particle momentum;

- energy deposited in the first layer of the hadron calorimeter does not exceed 25% of the charged particle momentum;

- total energy deposited in all calorimeters is less than 80% of the charged particle momentum.

The strong identification criteria for electrons were:

- momentum of the charged particle in the cluster exceeds 5 GeV/c;

- energy deposited in the electromagnetic calorimeter exceeds 60% of the cluster energy or 15 GeV;

- energy deposited in the first layer of the hadron calorimeter does not exceed 12 GeV;

- energy deposited beyond the first layer of the hadron calorimeter does not exceed 15% of the cluster energy and 2.5 GeV;

5

The soft identification criteria for electrons were:

- momentum of the charged particle in the cluster exceeds 15 GeV/c;

- particle is identified as a "very loose" electron by the standard DELPHI identification package [1];

- at least one hit in the vertex detector is associated with the track of the particle;

- energy deposited beyond the first layer of the hadron calorimeter does not exceed 15%;

The cuts applied on the discriminating variables for the different final states are given in table 1. The $e^+e^-q\bar{q}$ final state contains more background coming from wrong electron identification and from photon conversions. To suppress it the following additional criteria were used for this channel:

- at least one of the electron candidates had associated hits in the vertex detector;

- if P_t is less than 8 GeV/c both electron candidates have associated hits in the vertex detector;

- if P_t is less than 15 GeV/c the total energy of the photons included in the electron cluster does not exceed 30% of the momentum of the charged particle measured by the tracking system.

To select the on-shell Z^0Z^0 production the reconstructed masses of both the l^+l^- pair and the remaining hadronic system were required to be within 20 GeV/c² of the nominal Z^0 mass.

5.2   Results

The distribution of the mass of one fermion pair (l^+l^- or $q\bar{q}$) when the mass of the second pair is within 20 GeV/c² of the nominal Z^0 mass is shown in figure 1a,b. The distribution of the sum of masses of 2 fermion pairs is shown in figure 1c. The observed distributions are in reasonable agreement with the predictions from simulation.

The observed and predicted numbers of events with these selection criteria are shown in table 2. The background is divided into 2 parts: the first part comes from $l^+l^-q\bar{q}$ events outside the generation-level signal window and the second part comes from other processes, principally W^+W^-, other Z^0Z^0 decays and in the case of $e^+e^-q\bar{q}$, $q\bar{q}(+\gamma)$ production.

6 $\nu\bar{\nu}q\bar{q}$ Channel

The decay mode $\nu\bar{\nu}q\bar{q}$ represents 28% of the Z^0Z^0 final states. The signature of this decay mode is a pair of acoplanar jets with visible and recoil masses compatible with the Z mass. The analyzed data sample in this channel corresponds to a integrated luminosity of 155.3 pb^{-1}.

6

lepton identification criteria	P_t^{min} (GeV/c)	$(\chi^2/\text{NDF})_{max}$
μ strong - μ strong	4.0	15.0
e strong - e strong	5.0	8.0
μ strong - μ soft	6.0	5.0
e strong - e soft	9.0	4.0

Table 1: The selection criteria for different final states.

channel	data	MC tot.	MC signal	MC $l^+l^-q\bar{q}$ backgr.	MC other backgr.
$\mu^+\mu^- q\bar{q}$	6	4.55±0.49	4.02±0.47	0.39±0.15	0.14±0.04
$e^+e^- q\bar{q}$	2	4.54±0.39	3.69±0.35	0.71±0.16	0.14±0.04
Total	8	9.09±0.63	7.71±0.59	1.10±0.22	0.28±0.06

Table 2: The observed and expected number of selected $l^+l^-q\bar{q}$ events - candidates to the on-shell $Z^0 Z^0$ production. The errors shown are due to the simulation statistics only.

6.1 Selection procedure

6.1.1 Event variables

The iterated nonlinear discriminant analysis program (IDA) [13] was applied to calculate a second order polynomial from a set of event variables. The polynomial specifies a surface which maximizes the separation between signal and background in the event variable space, and its values can be used as weights for signal events. In order to use the combination of variables with the best performance, variables were selected one by one out of a large set of using an automatic procedure until no further improvement in the discrimination was obtained. The automatic procedure computed the second order discriminant for each variable in the set and selected the variable which together, with those already selected, gave the best discrimination power, defined as:

$$\lambda = \frac{N_b N_s}{(N_b + N_s)^2} \frac{(\mu_b - \mu_s)^2}{\sigma_{bs}^2}$$

where N_b and N_s are the normalized number of events, and μ_b and μ_s are the mean values of the second order polynomial for background and signal, respectively, and σ_{bs} is the variance for both together.

The hadronic jets were defined with the LUCLUS[4] routine. In some variables the event was forced into a two-jet configuration, otherwise jets were defined with the default scaled invariant mass parameter $y_{join} = m_{min}^2 / E_{vis}^2 = 0.05$.

The following nine variables were selected :

- $\theta(min, 15\%)$: The minimum polar angle defining cones in the positive and negative beam directions such that 15% of the total visible energy is contained in the cone. Large values of this variable characterized events with the main jet activity far away from the beam directions.

- Acoplanarity: the logarithm of the scaled acoplanarity. Acoplanarity is defined as $180°\text{-}\Delta\phi$, where $\Delta\phi$ is the difference in azimuthal angle between the total momentum vectors in the opposite event hemispheres. In order to compensate for the geometrical instability of this variable for jets pointing at low polar angles it was scaled by the sine of the minimum polar angle between momentum vectors and the beam axis;

- M_{rec}: The recoil mass of the hadronic system; a negative value was assigned if M_{rec}^2 was negative.

- E_{vis}/E_{cms}: the total reconstructed energy, scaled by the centre-of-mass energy;

- $max(P_T(jet))$: the maximum transverse momentum between any particle and a jet.

- E_γ/E_γ^Z: the normalized energy of a photon, assumed to have escaped in the beam direction, deduced from the polar angles of the two main jet directions in the event. The photon energy estimate was normalized to the energy expected for a photon recoiling against an on-shell Z in order to minimize the effect of small variations of the centre-of-mass energy in the data compared to simulation;

- E_{jet1}: the energy of the higher energy jet of the bi-jet system.

- $|\cos\theta_{P_{miss}}|$: cosine of the angle between the missing momentum and the nearest z-axis;

- Thrust: the thrust, computed in the rest frame of the visible system. The transformation into the rest frame is made in order to compensate for the smearing due to the boost of the jet system. This thrust variable defines a resolution of acoplanarity which is broader in spherical multijet events.

6.1.2 Preselections

Preselections were defined in three steps A, B and C. The agreement between data and simulation was checked at each step.

A: To select multihadronic annihilation events, the following criteria were applied:

- the number of charged particles should be at least nine;
- one or more charged tracks, with a transverse momentum larger than 1.5 GeV/c should extrapolate back to within 200 μm of the primary vertex, in the plane transverse to the beam axis;
- the total energy carried by charged particles should be greater than 0.1 E_{cms}.
- the mass of the visible system was required to be in the range 80±20 GeV/c^2. No rescaling was applied to the reconstructed mass at this stage.

B: Photon hermeticity

A veto algorithm based on the hermeticity counter signals was applied in order to reject events with an on-shell Z and a missing or poorly reconstructed photon at large polar angles. These scintillator counters were installed at polar angles of 90° (the

8

connection between two detector hemispheres) and 40° (the gap between the barrel and forward electromagnetic calorimeters) where a photon can escape undetected. The signals in the hermeticity counters were considered under the hypothesis of two jets with one photon lost in the beam pipe and another photon going in the direction of the taggers. If this was kinematically and topologically consistent, the event was rejected.

C: Signal Region Preselection

A loose selection based on the most discriminant variables was applied to define the signal region. The requirements are listed in table 3. The ratio of expected signal and background was of the order of 0.05 after this step.

The agreement between data and simulation rates for the signal channel and the background after each preselection step are shown in table 4. The data and simulation rates agree within 6% after steps A and B. The distributions of several event variables are shown for step C in figures 2 and 3. The observed and expected rates are within 1.5 σ of each other after step C.

Variable	lower cut	upper cut
$\theta(min, 15\%)$	0.25	-
Acoplanarity	-0.54	1.75
M_{rec}	61	127 GeV/c^2
E_{vis}/E_{cms}	0.33	0.56
$max(P_T(jet))$	0.58	9.2 GeV/c
E_γ/E_γ^Z	-	0.85
E_{jet1}	29	73 GeV
$\|\cos\theta_{P_{miss}}\|$	-	0.98
Thrust	0.74	-

Table 3: Preselection step C for channel $\nu\bar{\nu}q\bar{q}$.

6.1.3 Discriminant functions and mass reconstruction

The simulated events passing preselection C were used for calculating the first IDA function which has a distribution shown in figure 4a; the expected distribution for the signal is shown in figure 4b. As input for the second iteration a cut was applied keeping 80% of the signal.

The distribution of the weight after the second iteration is shown in figure 4c); the expected distribution for the signal is shown in figure 4d). The weight distributions as well as the signal and background predictions were obtained from simulation samples that were statistically independent of the samples used in computing the IDA functions.

Estimates of the invariant mass of the q$\bar{q}$-system were reconstructed by using the visible masses. In the rescaling formula, the energy and momentum were required to be conserved and the invariant mass of the recoil system was constrained to the Z mass. The

9

| Selection | Data | total MC | $\nu\bar{\nu}q\bar{q}$ | | CC 4-f | $q\bar{q}\gamma$ | $q\bar{q}\ell\bar{\ell}$ | $\gamma\gamma$ |
Selection			signal	bkg.				+bhabha
Step A	6770	6390±30	23.1±0.3	0.9±0.1	378±3	5553±9	19.3±1.2	417±28
Step B	6395	6025±29	20.9±0.3	0.9±0.1	339±3	5264±9	18.3±1.2	383±27
Step C	416	381±4	18.7±0.3	0.5±0.1	114±2	242±2	1.3±0.3	6±3
1st IDA	59	49±1	15.2±0.3	0.13±0.04	22.8±1.1	10.8±0.5	0.3±0.1	0

Table 4: $\nu\bar{\nu}q\bar{q}$ channel: Data and simulation rates after different steps of the analysis. The uncertainties are simulation statistics. The $\nu\bar{\nu}q\bar{q}$ background refers to $\nu\bar{\nu}q\bar{q}$ events outside the generator-level mass window. The CC 4-f background refers to charged-current four-fermion processes such as W^+W^-.

reconstructed mass can be expressed as:

$$M_{q\bar{q}} = \frac{E_{\mathrm{cms}}E_{\mathrm{vis}} - \sqrt{E_{\mathrm{cms}}{}^2 E_{\mathrm{vis}}{}^2 - M_{\mathrm{vis}}{}^2 \left(E_{\mathrm{cms}}{}^2 - m_{\mathrm{Z}}{}^2\right)}}{M_{\mathrm{vis}}}$$

The distribution of the reconstructed mass is shown in figure 4e).

The efficiencies and expected number of standard model events and data are summarized in table 4.

6.2   Results

The selected data sample at this final preselection level consisted of 59 events. The background and signal predictions are 34±1 and 15.2±0.3(stat.). The largest background contributions come from charged-current four-fermion processes like W^+W^- production.

Imposing a cut on the IDA output to obtain a signal-to-background ratio of 3, 6 events were found compared with the predicted signal of 5.7 events and predicted background of 2.0 events.

7 $b\bar{b}q\bar{q}$ Channel

The $Z^0Z^0 \to q\bar{q}q\bar{q}$ process produces four or more jets in the final state. However, W^+W^- and QCD processes can also produce such final states and since the cross-sections for these processes are orders of magnitude greater than the Z^0Z^0 cross-section, powerful signal identification techniques are necessary to enrich the purity of the sample. This analysis is directed towards final states in which one of the on-shell Z^0 decays into $b\bar{b}$ since b quarks are only rarely produced in W^+W^- events.

7.1   Selection of hadronic Z^0Z^0 events

The aim of the four jet preselection is to eliminate radiative and $\gamma\gamma$ events and to reduce the QCD and $Z^0\gamma^*$ background. In each event, the following requirements were imposed:

- at least 19 charged particles in the event;

	Signal	$Z^0\gamma^*$	QCD	W^+W^-	MC	$DATA$
Presel. cuts efficiencies	38%	22%	3.7%	41%		
Exp. nb of evts	38.9	28.7	607.6	1038.4	1708.5	1679
Final selection	3.9	0.14	0.95	0.26	5.3	6

Table 5: Efficiencies and number of events selected in the $b\bar{b}q\bar{q}$ channel after preselection cuts for an integrated luminosity of $158pb^{-1}$. The branching fractions of Z^0 and W^+, W^- bosons into hadronic final states has already been included. The last line gives the number of events selected after a cut on the discriminant variable.

- visible energy of the event at least $60\%\sqrt{s}$;

- the sum of the energies of neutral particles in the event less than $50\%\sqrt{s}$;

- the sum of all energy deposits in the electromagnetic calorimeters, whether or not those deposits were associated with a charged particle, was required to be less than 30 GeV;

- the energy of any identified photon has to be smaller than 30 GeV;

- the Fox-Wolfram moments of order two and four were required to be less than 1.1;

- the charged and neutral particles were clustered using the Durham jet algorithm[15] and forced into a four jet configuration. At least one charged particle was required to be present in each jet and the mass of each jet was required to be at least 1.5 GeV/c^2.

The efficiencies for selecting the signal and background channels using this preselection were estimated using simulated events and are shown in table 5. In this table, signal refers to $b\bar{b}q\bar{q}$ events with masses inside the 10 GeV/c^2 generator-level mass window (a small contribution from $c\bar{c}q\bar{q}$ is also included). $Z^0\gamma^*$ is here taken to include $b\bar{b}q\bar{q}$ events outside the generator-level mass window.

7.2   Mass Reconstruction

The main purpose of the mass reconstruction in the four-jet channel was to help discriminate against background sources, particularly $q\bar{q}(+n\gamma)$. To achieve this the ambiguity in the pairing of the four jets has to be resolved. To this end, the four-momenta of the four jets were fitted by using a five constraint kinematic fit. In addition to energy-momentum conservation applied to the whole event, one of the dijet masses was required to be equal to the Z-mass. Six different pairings were obtained. This analysis examines four-jet events in which a Z^0 decays into a $b\bar{b}$ pair. Therefore, b-quark tagging[16] was used together with the information from the kinematic fit to select the pairing which had the highest probability of being produced by $Z^0 \rightarrow b\bar{b}$. A likelihood was constructed combining the χ^2 probability of the 5C fit and the probabilities that the two jets are b-jets; the combination of jets with the highest likelihood was selected as a Z^0 candidate. The mass of the system formed by the other two jets was then computed (see figure 5) and its value used to estimate the mass of the second Z^0 candidate.

7.3 Discriminant Analysis

Events originating from the signal and from the background were separated using the value of a discriminant variable. This variable combined the information from shape variables to reduce the QCD background and from the b-tagging variables to reduce the contribution of W^+W^- pairs.

- **The shape variables**
  These variables were : the minimum di-jet mass; $\alpha_{min}.E_{min}$, the product of the minimum jet energy and the minimum opening angle between two jets; $(H_2 + H_4)/H_0$, the normalized sum of Fox-Wolfram moments; $\beta_{min}.E_{max}/E_{min}$, where β_{min} is the minimum angle between the most energetic jet, of energy E_{max}, and the others; the value of the cut in the jet algorithm, y_{34}, corresponding to the transition between three and four jets topologies for the studied event.

- **The b-tagging variable**
  The most effective variable against W^+W^- background was found to be the combined b-tagging probability measured for each jet (as discussed in [16]).

The distributions of these variables were fitted and the corresponding functions used to construct the final discriminant variable. The distant tails in these distributions were replaced by a constant level. The discriminant variable was predicted using simulated events, taking as signal those Z^0Z^0 events in which at least one Z^0 decayed into $b\bar{b}$. The background was subdivided into QCD and W^+W^- events. For these three populations a probability combining kinematics, b-tagging and topological properties was evaluated. The discriminant variable was then taken to be the ratio between the probabilities for signal and background hypotheses (See figure 6).

7.4 Results

Imposing a cut on the discriminant variable together with a cut on the reconstructed mass of the second Z^0 candidate at 80 GeV/c^2 to obtain a signal-to-background ratio of 3, 6 events were observed, compared with a predicted signal of 3.5 events and a predicted background of 1.4 events.

8 Extraction of NC02 cross-section and Conclusions

The observed and predicted numbers of events in each channel are summarized in table 6. For those channels where a discriminant variable was used ($\nu\bar{\nu}q\bar{q}$ and $b\bar{b}q\bar{q}$), a cut was made at a signal-to-background ratio of 3. The value of the conversion factor R (defined in eq. (1)) used to convert from the observed four-fermion cross-section in the mass window to the total NC02 cross-section is given for each channel. Note that for the $e^+e^-q\bar{q}$ channel the R factor is less than one: this is due to significant extra contributions from diagrams other than NC02 such as $Z^0e^+e^-$. The R factor is not given for the $l^+l^-l^+l^-$ channel because the prescription of eq. (2) was used instead.

The distribution of the sum of the Z^0 boson candidate masses is shown in figure 7, derived as the sum of the two Z^0 masses for all of the candidates accepted in each of the five channels. The observed mass distribution is in good agreement with the predicted distribution which is also shown in the figure.

Channel	data	N_{total}	N_{signal}	$N_{background}$	R
$l^+l^-l^+l^-$	1	0.9	0.6	0.3	-
$e^+e^-q\bar{q}$	2	4.5 ± 0.4	3.7 ± 0.4	0.8 ± 0.2	0.88
$\mu^+\mu^-q\bar{q}$	6	4.5 ± 0.4	4.0 ± 0.5	0.5 ± 0.2	1.05
$\nu\bar{\nu}q\bar{q}$	6	7.7 ± 0.5	5.7 ± 0.3	2.0 ± 0.4	1.05
$b\bar{b}q\bar{q}$	6	4.9	3.5	1.4	1.14
Total	21	22.5	17.5	5.0	-

Table 6: Number of events selected and predicted (total, signal and background) for the different channels and the conversion factor R used to translate between the observed four-fermion cross-section and the NC02 cross-section. Errors, where quoted, are from simulated statistics only.

The observed and predicted numbers of events were then used in a maximum likelihood fit to the Poisson probability of observing a given number of events for various values of the NC02 cross-section, constraining the branching ratios of the Z^0 to those in [10]. The value for the NC02 cross-section so obtained was:

$$\sigma_{NC02} = 0.58 \pm 0.17 \ pb, \tag{3}$$

where the quoted error is statistical only. This is in good agreement with the Standard Model prediction from EXCALIBUR of 0.64 pb.

Acknowledgements

References

[1] DELPHI Collaboration, P.Abreu et al., Nucl. Instr. and Meth. **A378** (1996) 57.

[2] DELSIM Reference Manual, DELPHI 87-97 PROG-100

[3] F.A. Berends, R. Pittau, R. Kleiss, Comp. Phys. Comm. **85** (1995) 437.

[4] T. Sjöstrand, Comp. Phys. Comm. **39** (1986) 347; T. Sjöstrand, PYTHIA 5.6 and JETSET 7.3, CERN-TH/6488-92.

[5] Y.Kurihara, J. Fujimoto, T. Munehisa, Y. Shimizu, KEK CP-035, KEK 95-126 (1995).

[6] E. Accomando, A. Ballestrero Comp. Phys. Comm. **99** (1997) 270

[7] Y. Kurihara et al., Vol. 2 30 2 45 in Physics at LEP2 G. Altarelli, T. Sjöstrand and F. Zwirner (eds.) CERN 96-01 (1996)

[8] S.Nova, A.Olshevski, and T. Todorov, *A Monte Carlo event generator for two photon physics*, DELPHI note 90-35 PROG 152.

[9] F. A. Berends, P. H. Daverveldt, R. Kleiss, Comp. Phys. Comm. **40** (1986) 271-284, 285-307, 309.

[10] Particle Data Group, Eur. Phys. **C3** (1998)

[11] T. Sjöstrand, Comp. Phys. Comm. **28** (1983), 229.

[12] see section 5.2 in P. Abreu *et al.* E. Phys. J. **C2** (1998) 581.

[13] T.G.M. Malmgren, Comp. Phys. Comm. **106** (1997) 230;
T.G.M. Malmgren and K.E. Johansson, Nucl. Inst. Meth. **403** (1998) 481.

[14] DELPHI collaboration, P.Abreu *et al.*, *Search for neutral Higgs bosons in e^+e^- collisions at $\sqrt{s} = 183$ GeV* DELPHI 98-95 CONF 163 (submitted to ICHEP98 conferences).

[15] S. Catani, Yu.L. Dokshitzer, M. Olson, G. Turnock and B.R. Webber Phys. Lett. **B269** (1991) 432.
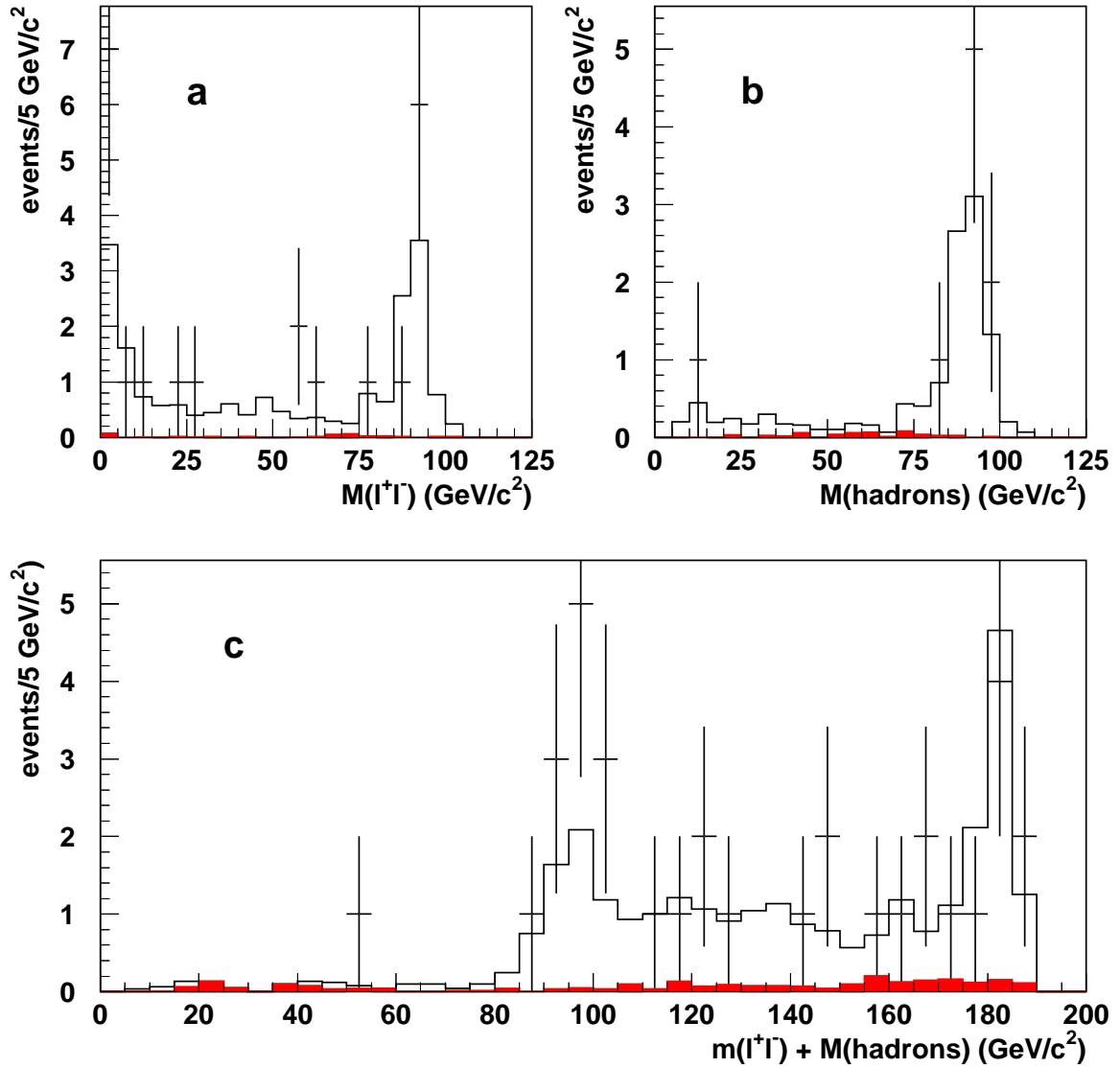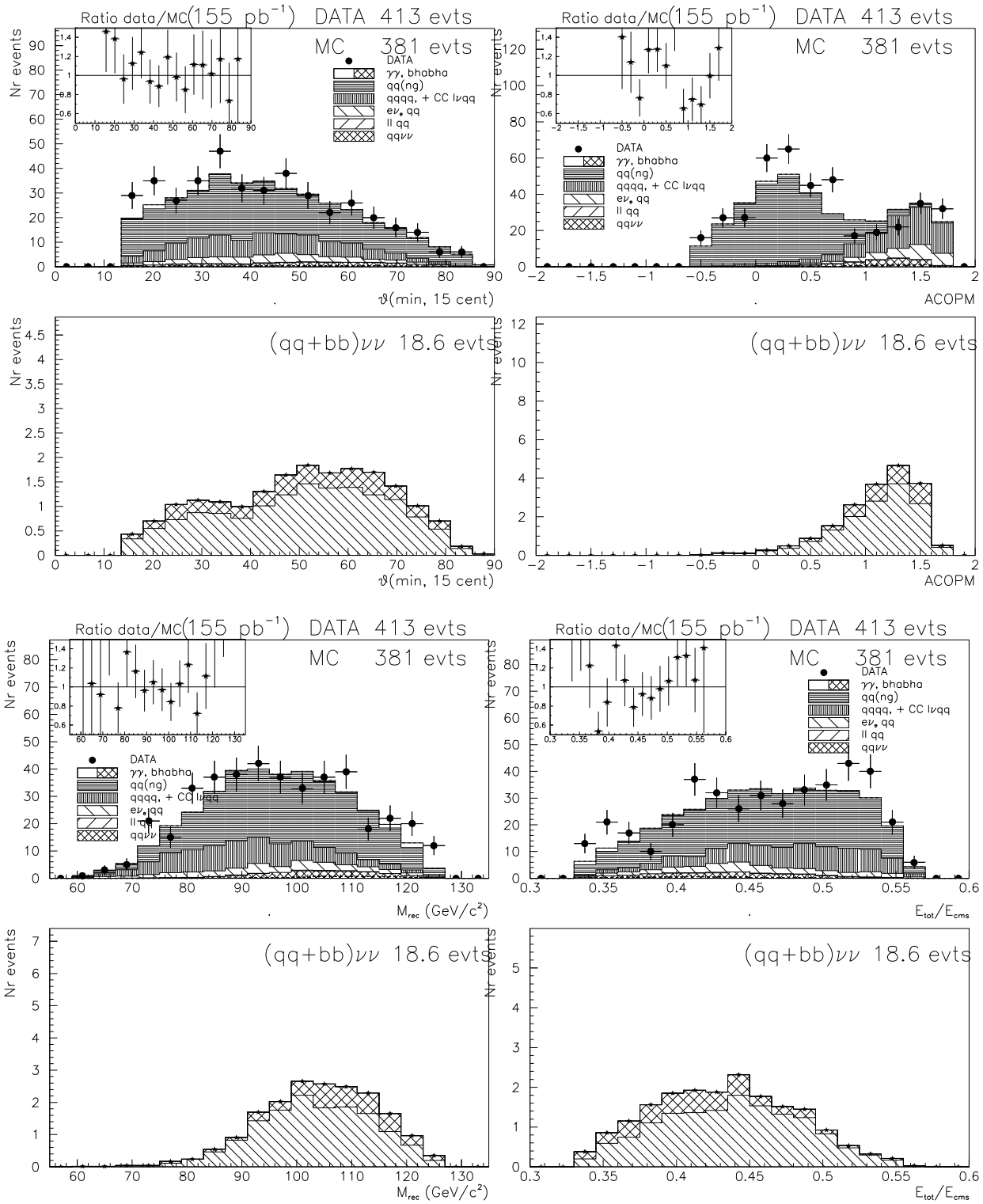
[16] G.Borisov, Nucl. Instr. Meth. **A417** (1998), 384

Figure 1: a) - the distribution of the mass of the l^+l^- pair when the mass of the hadron system is within 20 GeV/c^2 of the nominal Z^0 mass; b) - the distribution of the mass of the hadron system when the mass of the l^+l^- pair is within 20 GeV/c^2 of the nominal Z^0 mass; c) - the distribution of the sum of masses of the l^+l^- pair and the hadron system. The points are the data, the histogram is the simulation prediction and the filled histogram is the contribution of the background.
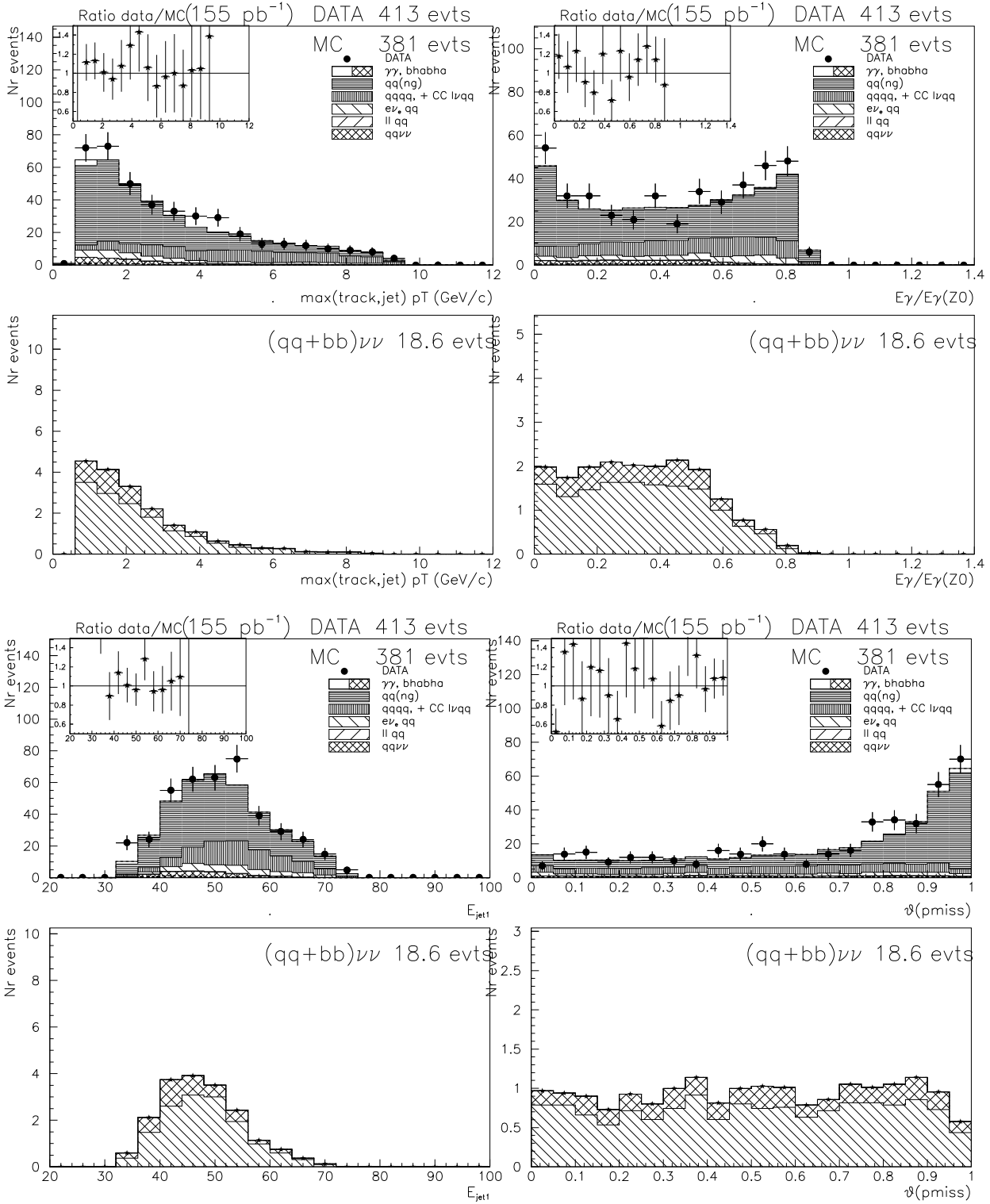
Figure 2: **DELPHI PRELIMINARY**. A comparison of data (dots) and simulation for various event variables after the preselection C for channel $\nu\bar{\nu}q\bar{q}$. For each variable, the distribution of the expected signal (light flavour quarks hatched, beauty cross-hatched) is shown in the lower window. The definitions of the variables are given in the text.

16

Figure 3: **DELPHI PRELIMINARY**. As in figure 2, but for different variables, as defined in the text.

a)

b)

c)

d)

e)
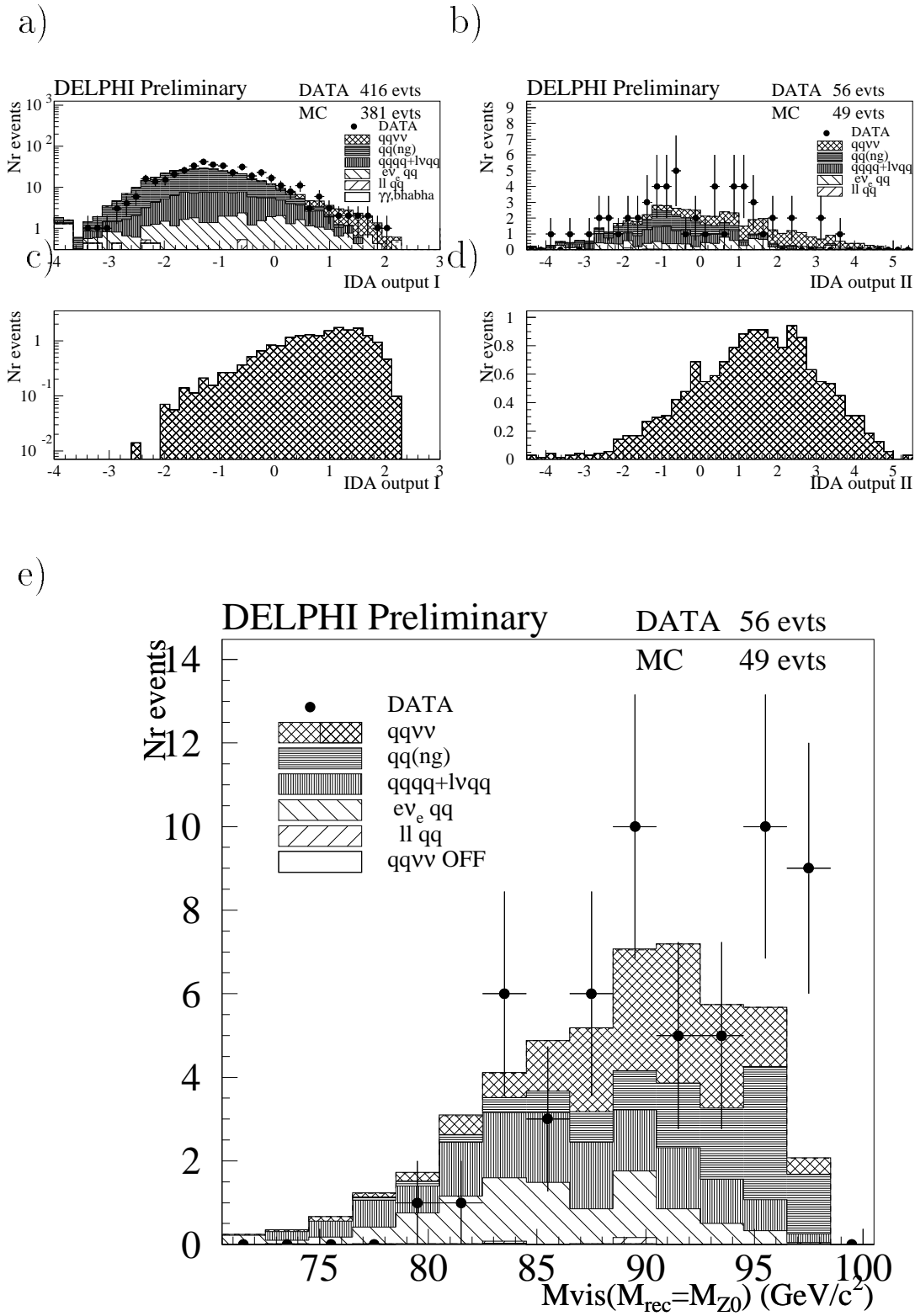
Figure 4: **DELPHI PRELIMINARY**. The weight outputs of the iterative discriminant analysis (IDA) for channel $\nu\bar{\nu}q\bar{q}$. The data (points) and prediction from simulation from various sources (shaded histograms) are shown for the first IDA function (a), the second IDA function (b), the signal distribution of the first IDA function (c), and the second IDA function(d). The distribution of the reconstructed mass of the $q\bar{q}$ -system is shown in e).
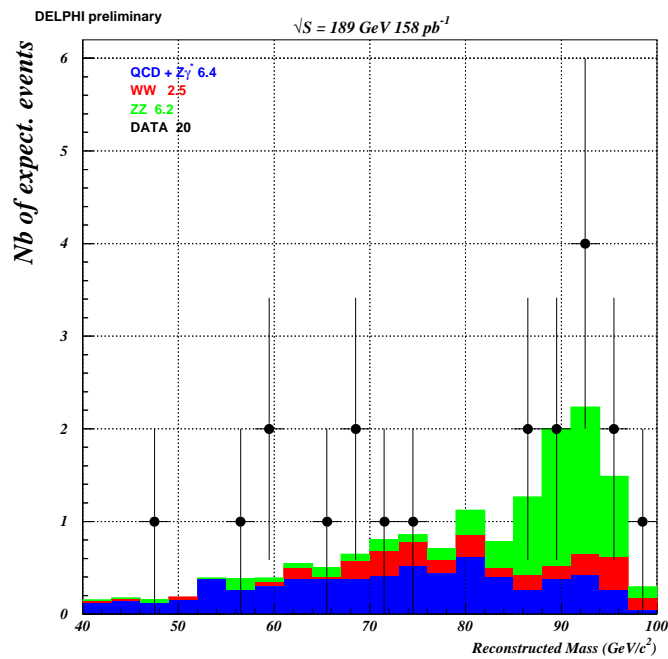
Figure 5: **DELPHI PRELIMINARY**. The reconstructed mass of the $q\bar{q}$ candidates in the $b\bar{b}q\bar{q}$ channel. The points are the data, the histogram is the simulation with different shadings used to indicate the different sources of events in the simulation. Relaxed cuts corresponding to a signal-to-background ratio of 1 were used.
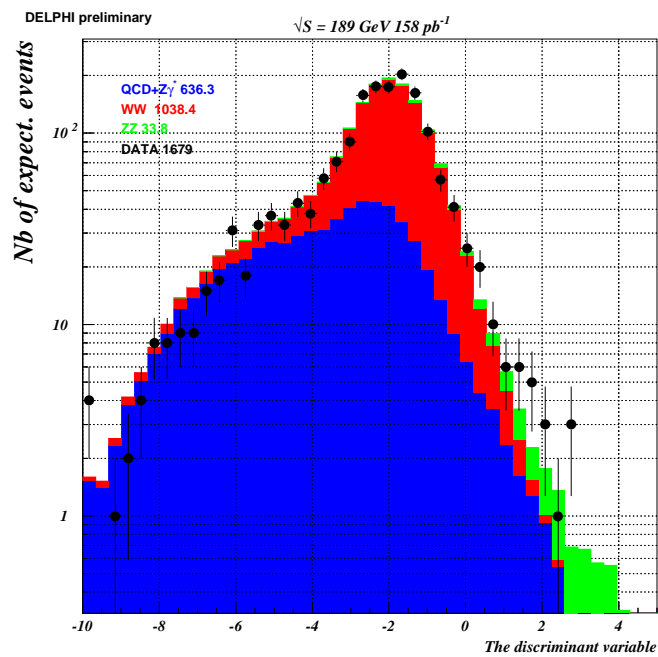
Figure 6: **DELPHI PRELIMINARY**. The discriminant variable for events selected by the preselection cuts in data (points) and simulation(histogram) with the contributions from different sources shown with different shadings for the $b\bar{b}q\bar{q}$ channel.
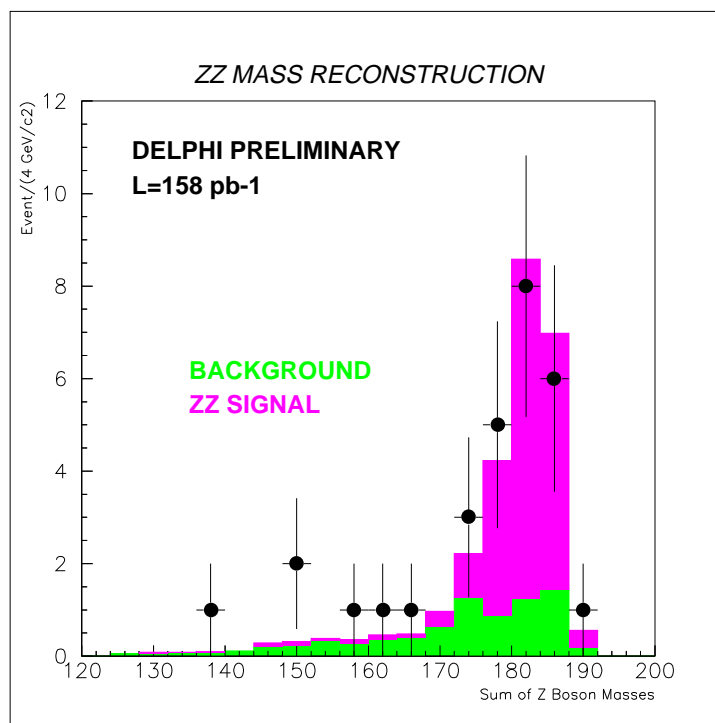
Figure 7: **DELPHI PRELIMINARY**. The sum of the masses of the two Z boson candidates in all channels for the data (points) and the simulation (histogram).